

Kinetic and Thermodynamic Characterization of Camptothecin Hydrolysis at Physiological pH in the Absence and Presence of Human Serum Albumin

RISHI THAKUR, SASANK KUNADHARAJU, MICHALAKIS SAVVA

Division of Pharmaceutical Sciences, Arnold & Marie Schwartz College of Pharmacy & Health Sciences, Long Island University, Brooklyn, NY 11201

Received 3 February 2009; revised 26 April 2009; accepted 22 May 2009

DOI 10.1002/kin.20449

Published online in Wiley InterScience (www.interscience.wiley.com).

ABSTRACT: To accurately derive the kinetic and thermodynamic parameters governing the hydrolysis of the lactone ring at physiological pH, a derivative spectrophotometric technique was used for the simultaneous estimation of lactone and carboxylate forms of camptothecin (CPT). The hydrolysis of the CPT-lactone and the lactonization of CPT-carboxylate at 310.15 K followed a first-order decay with apparent rate constants equal to $0.0279 \pm 0.0016 \text{ min}^{-1}$ and $0.0282 \pm 0.0024 \text{ min}^{-1}$, respectively. The activation energy associated with the hydrolysis of the CPT-lactone and the lactonization of the CPT-carboxylate as calculated from the Arrhenius equation was 89.18 ± 0.84 and $86.49 \pm 2.7 \text{ kJ mol}^{-1}$, respectively. The enthalpy and entropy of the thermodynamically favored hydrolysis reaction were on average $10.49 \text{ kJ mol}^{-1}$ and $48.00 \text{ J K}^{-1} \text{ mol}^{-1}$, respectively. The positive enthalpy and entropy values of the CPT-lactone hydrolysis indicate that the reaction is endothermic and entropically driven. The stability of CPT-lactone in the presence of human serum albumin (HSA) was also analyzed. Notwithstanding the much faster hydrolysis of the CPT-lactone in the presence of HSA at various temperatures, the energy of activation was determined to be similar to the one estimated in the absence of HSA, suggesting that HSA does not catalyze the hydrolysis reaction, but it merely binds, sequesters, and stabilizes the CPT-carboxylate species. © 2009 Wiley Periodicals, Inc. *Int J Chem Kinet* 41: 704–715, 2009

INTRODUCTION

Fifty years have past since the discovery of the topoisomerase I inhibitor, camptothecin (CPT) was publicly announced, and still its fast hydrolysis in the blood

Correspondence to: Michalakis Savva; e-mail: msavva@liu.edu.
© 2009 Wiley Periodicals, Inc.

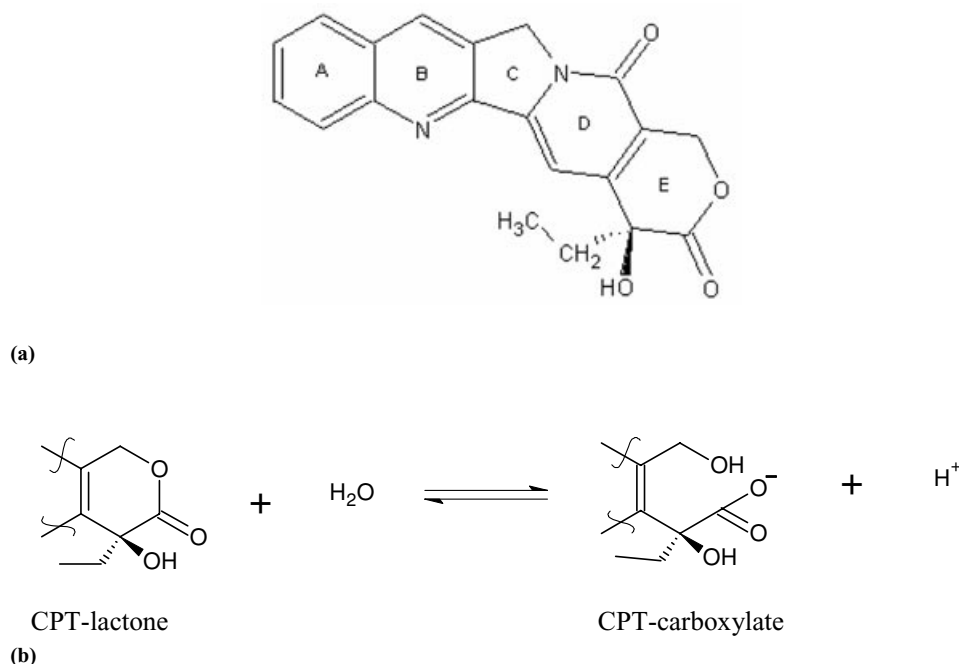


Figure 1 (a) Chemical structure of CPT. (b) The reversible hydrolysis reaction of CPT-lactone (C₂₀H₁₆N₂O₄) to CPT-carboxylate (C₂₀H₁₇N₂O₅). The forward direction of the reaction is shown from left to right. The reverse direction of the reaction is the thermodynamically unfavorable esterification of the CPT-carboxylate species at pH 7.4.

precludes its efficient delivery [1–4]. The α -hydroxy δ -lactone moiety of CPT (Fig. 1), which is structurally important for the drug interaction with topoisomerase I and passive diffusion of CPT into cancer cells, undergoes a pH-dependent reversible hydrolysis at and above pH 5 to a ring-opened carboxylate form. Thus, the hydrolysis product of CPT, referred herein as CPT-carboxylate, is quickly produced in the blood or in aqueous media of neutral pH and is reported to be of reduced activity, bioavailability, and the cause of toxic side effects in human trials [5–8].

The hydrolysis kinetics of the CPT and its analogues at physiological pH and at ambient temperature have been reported in many publications, but the thermodynamic parameters governing this important hydrolysis reaction have not yet been reported [6–10] except for the 10-hydroxy camptothecin, which we have recently completed [11]. This investigation is a continuation of our recent study highlighting the superiority of first derivative spectroscopy, a real-time nonperturbing method developed in our laboratory for the simultaneous determination of nonequilibrium concentrations of CPT, lactone (CPT-lactone) and carboxylate (CPT-carboxylate) species at various temperatures. The technique was also very useful in assessing the stability of CPT in the presence of human serum albumin (HSA), thus demonstrating the potential of this technique in CPT delivery system selection. The kinetic and thermo-

dynamic analysis of the data presented herein has revealed new information regarding the stability of CPT in the presence and absence of HSA.

MATERIALS AND METHODS

Explanation of Terms

The terms CPT, CPT-lactone, and lactone are used interchangeably throughout the article and denote the native lactone form of the CPT. The term CPT-carboxylate denotes the hydrolysis product of the native CPT-lactone molecule. Moreover, the term *forward direction* of the reversible hydrolysis reaction denotes the hydrolysis of the CPT-lactone and has as reactants and products CPT-lactone and CPT-carboxylate, respectively. The term *reverse direction* of the hydrolysis reaction denotes the esterification or lactonization of CPT-carboxylate and has as reactants and products CPT-carboxylate and CPT-lactone, respectively. The term lactonization reaction is used when the starting material is CPT-carboxylate. The *forward direction* of the lactonization reaction denotes the lactonization of the CPT-carboxylate and has as reactants and products CPT-carboxylate and CPT-lactone, respectively, whereas the term *reverse direction* of the lactonization reaction denotes the hydrolysis of CPT-lactone.

Finally, kinetic experiments performed with CPT-lactone as the starting material are referred to as hydrolysis reaction, whereas measurements collected with CPT-carboxylate as the starting material are referred to as lactonization or esterification reaction, albeit lactone hydrolysis is the spontaneous or thermodynamically favorable reaction.

Materials

The 20(*S*)-(+)-camptothecin (4-ethyl-4-hydroxy-1H-pyrano-(3',4':6,7) indolizino (1,2-*b*)quinoline-3,14-(4*H*,12*H*)-dione (CAS Number 7689-03-4), C₂₀H₁₆N₂O₄, 348.352 g mol⁻¹, stated mass fraction purity ≥0.99 was purchased from LC Laboratories (Woburn, MA). In close agreement with the vendor's stated purity, our elemental analysis of CPT-lactone yielded a mass fraction purity of 0.99 (Calcd: C, 68.96; N, 8.04; H, 4.63. Found: C, 68.87; N, 8.20; H, 4.58; Robertson Microlit Laboratories, Madison, NJ). In addition, HPLC analysis of the CPT using fluorescence detector did not show any presence of related impurities (data not shown). All experiments were performed using analytical-grade reagents without further purification. Deionized water for preparation of buffer solutions was obtained from Barnstead NANO pure water system (Barnstead, Dubuque, IA). Dimethyl sulfoxide (DMSO) and sodium hydroxide (1 N) were purchased from Sigma-Aldrich (St. Louis, MO). The CPT-lactone stock solutions were prepared in DMSO at 2.871 × 10⁻⁴ M concentration. The CPT-carboxylate stock solutions were prepared in 0.001 N NaOH at concentration of 5.741 × 10⁻⁵ M from the CPT-lactone stock solutions in DMSO and equilibrated for 1 h at room temperature to ensure complete hydrolysis (HPLC analysis, data not shown). PBS (0.137 M NaCl, 0.0027 M KCl, 0.010 M Na₂HPO₄, 0.002 M KH₂PO₄) was used to maintain the pH at 7.4. HSA, 66478 Da, CAS Number: 70024-90-7, fraction V, stated mass fraction purity ≥0.96 was purchased from Sigma-Aldrich.

Fluorescence Measurements

Zero-time excitation scans of CPT-lactone and carboxylate were recorded within 20 s of stock dilution and used as reference spectra of the pure CPT-lactone or pure CPT-carboxylate (Fig. 1b), on a Cary Eclipse fluorescence spectrophotometer (Varian Inc., Victoria, Australia), as described elsewhere [11]. The effect of DMSO on the spectral properties of lactone was safely neglected as the volume fraction of DMSO was less than 1%. Scans of either pure CPT-lactone or CPT-carboxylate were collected at pH 7.4

by diluting the respective stocks in 3 cm³ quartz cuvettes to give a final concentration of 8.612 × 10⁻⁷ M. First-order derivatives of the spectral excitation scans were used to determine the zero-crossing points (λ_{ZCP}) of pure CPT-lactone and CPT-carboxylate at 363 and 369 nm, respectively (Fig. 2). In the presence of HSA, a bathochromic shift of the zero-crossing points was observed at 369 and 379 nm, respectively (not shown).

Kinetic Investigation of the Hydrolysis and Lactonization Reactions

Kinetic measurements were performed by approaching the equilibrium from both directions of the reaction, as described elsewhere [11]. Briefly, to determine the reaction kinetics of the hydrolysis reaction, the buffer solution was preequilibrated to the desired temperature and an aliquot of CPT-lactone from the DMSO stock solution was added to give the final concentration of 8.612 × 10⁻⁷ M. The excitation scans were collected immediately and at different time intervals (1.0–5.0 min), thereafter, depending on the rate of the reaction. The percent CPT-lactone remaining at each time interval was determined at the λ_{ZCP} of the CPT-carboxylate and vice versa. The stability and hydrolysis kinetics of CPT-lactone in the presence of HSA (3.008 × 10⁻⁴ M) in PBS (pH 7.4) at narrow temperature range (298.15–314.25 K) were analyzed similarly. The reaction kinetics of the lactonization reaction was also monitored, starting with 100% CPT-carboxylate at zero time.

Kinetic Parameters

The exponential decay of CPT-lactone versus time was fitted using Eq. (1) by the method of nonlinear least squares with [CPT-lactone]_{eq}, [CPT-carboxylate]_{eq}, and k_{obs} being the adjustable parameters.

$$[\text{CPT-lactone}] = [\text{CPT-lactone}]_{eq} + [\text{CPT-carboxylate}]_{eq} \cdot e^{-k_{obs} \cdot t} \quad (1)$$

The [CPT-lactone], [CPT-lactone]_{eq}, and [CPT-carboxylate]_{eq} are the concentrations of CPT-lactone at time t , the CPT-lactone at equilibrium, and the CPT-carboxylate at equilibrium, respectively, whereas k_{obs} is the overall or the observed first-order rate constant of the hydrolysis reaction.

It is to be noted that

$$k_{obs} = k_f + k_r \quad (2)$$

where k_f and k_r are the forward or hydrolysis and the reverse or lactonization rate constants, respectively, of

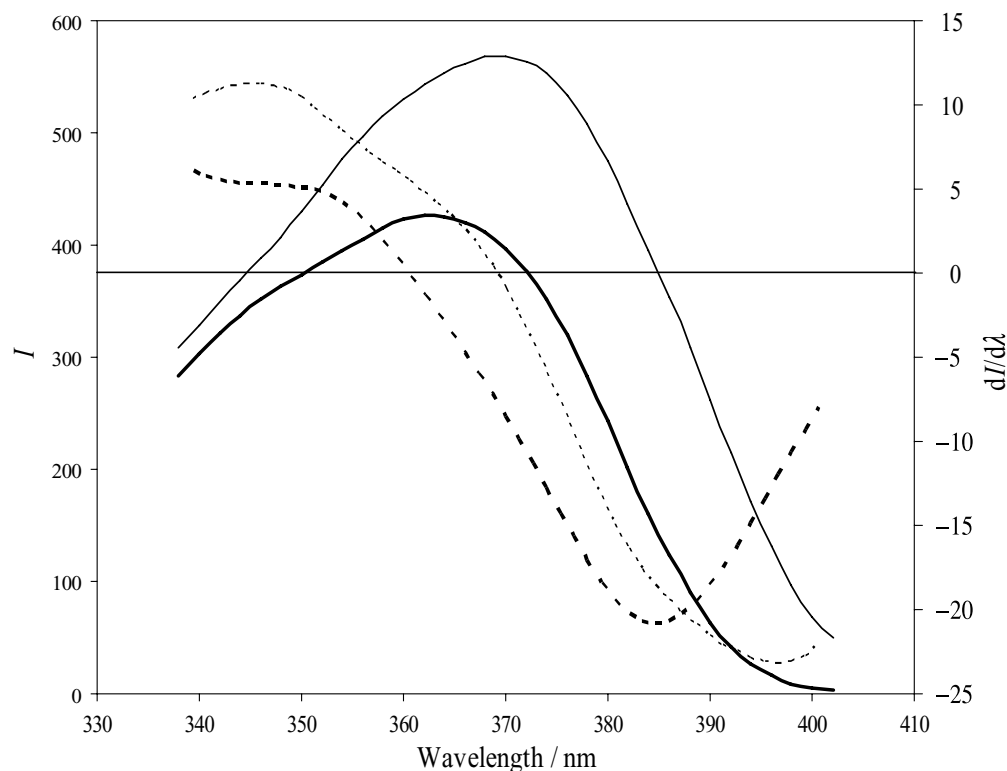


Figure 2 Representative excitation scans of CPT-lactone (—) and CPT-carboxylate (—) and their respective first derivative scans (thick and thin dashed lines) at temperature and pH of 304.15 K and 7.4, respectively. The primary y-axis represents the intensity (I), and the secondary y-axis represents ($dI/d\lambda$) plotted against wavelength. The zero-crossing point $\lambda_{(ZCP)}$ is defined as the wavelength at which the first derivative of the spectra is zero. The concentration of the CPT-lactone and the CPT-carboxylate was kept constant at 8.612×10^{-7} M.

the hydrolysis reaction. Since the reaction being studied is a reversible reaction with both reactants and products being present at equilibrium, the apparent equilibrium constant of the hydrolysis reaction K'_h can be defined as

$$K'_h = \frac{k_f}{k_r} = \frac{[\text{CPT-carboxylate}]_{\text{eq}}}{[\text{CPT-lactone}]_{\text{eq}}} \quad (3)$$

where $[\text{CPT-lactone}]_{\text{eq}}$ and $[\text{CPT-carboxylate}]_{\text{eq}}$ are the measured molar concentrations of CPT-lactone and CPT-carboxylate, respectively, at equilibrium. Similarly, the apparent chemical equilibrium constant of the lactonization reaction K'_l is defined as

$$K'_l = \frac{1}{K'_h} = \frac{k'_r}{k'_f} = \frac{[\text{CPT-lactone}]_{\text{eq}}}{[\text{CPT-carboxylate}]_{\text{eq}}} \quad (4)$$

where k'_f and k'_r are the forward or lactonization and the reverse or hydrolysis rate constants, respectively, of the lactonization reaction. The overall or observed rate of the lactonization reaction k'_{obs} is equal to $k'_f + k'_r$.

Recognize that both k_f and k'_r denote the true hydrolysis rate constant of the CPT-lactone calculated by monitoring the kinetics of the reversible hydrolysis and lactonization reactions, respectively, whereas k_r and k'_f denote the true lactonization rate constant of the CPT-carboxylate.

Given a $\text{p}K_a$ of the carboxylate species ~ 4 , the $[\text{CPT-carboxylate}]_{\text{eq}}$ is present almost exclusively in its ionized form at pH 7.4 [12]. The concentration of H_2O was not used in the calculation of the apparent equilibrium constant. The values of K'_h and k_{obs} were determined by direct nonlinear fitting of the experimental data by Eq. (1) using the Microsoft Excel Solver through minimization of the sum of the squared residuals at a 5% tolerance level. Subsequently, the rate constants k_f and k_r were calculated by solving Eqs. (2) and (3).

Thermodynamic Parameters

The temperature dependence of the rate constants was employed to calculate the activation energy by

using the integrated form of the Arrhenius equation, $k = A \cdot e^{-(E_a/RT)}$, where A is the frequency factor of the reaction. The rate constant k was determined at five different temperatures ranging from 304.15 to 329.15 K. Plots of $\ln k$ against the reciprocal of the corresponding absolute temperature were linear with a correlation coefficient greater than 0.998. From the slope and intercept of the linear fit, the activation energy and preexponential factor of CPT-lactone hydrolysis in the absence and presence of HSA and esterification of CPT-carboxylate were calculated.

The standard Gibbs free energy of the reaction was calculated from $\Delta_r G^\circ(T) = -RT \cdot \ln\{K'(T)\}$, where K' is the apparent chemical equilibrium constant of either the hydrolysis or the lactonization reaction. To verify the reliability of the thermodynamic parameters, the absolute values of $\Delta_r G^\circ(T)$ for the hydrolysis and lactonization reactions were compared and the difference was found to be statistically insignificant (95% confidence interval). The standard enthalpy and entropy of the reaction were determined from the slope and intercept of the integrated form of the Van't Hoff equation, which was used to model the data:

$$R \ln\{K'(T)\} = \Delta_r S^\circ(T) - \Delta_r H^\circ(T) \cdot \frac{1}{T} \quad (5)$$

Quantum Yield Study

Fluorescence quantum yield of CPT-lactone and CPT-carboxylate in the presence and absence of 3.008×10^{-4} M HSA in PBS buffer (pH 7.4) at 298.15 K was determined using quinine sulfate in 0.1 M H_2SO_4 as the reference with a quantum yield of $\phi = 0.545$ [13].

UV-vis absorbance spectra of dilute solutions (absorbance <0.05) of the two molecules were collected in reference to the corresponding solvents upon excitation at 350 nm on a Cary 50 UV spectrophotometer (Varian, Inc., Palo Alto, CA), whereas the corrected fluorescence spectra were recorded in the wavelength region of 371–600 nm using a Cary Eclipse fluorescence spectrophotometer. The 350-nm absorbances and the areas under the respective emission spectra of quinine sulfate and CPT-lactone and carboxylate species in the absence and presence of HSA were used to calculate the quantum efficiency (ϕ) of CPT species by Parker's method [14]:

$$\phi_u = \left(\frac{\phi_s \cdot m_u}{m_s} \right) \left(\frac{\eta_u^2}{\eta_s^2} \right) \quad (6)$$

where s and u represent the standard and unknown samples, whereas ϕ , m , and η are, respectively, the quantum yield, slope as obtained from the plots of inte-

grated fluorescence peak area against absorbance, and refractive index. The refractive index of 0.1 M H_2SO_4 ($\eta = 1.3335$), PBS ($\eta = 1.3340$), and PBS + HSA ($\eta = 1.3370$) were measured by a Bausch & Lomb refractometer (type 33.44.68). Plots of integrated fluorescence against the corresponding absorbance were linear with a correlation coefficient greater than 0.99.

RESULTS AND DISCUSSION

The first derivative spectroscopy using the zero-crossing technique was recently proved to be a powerful tool to resolve the overlapping spectra of 10-hydroxy-CPT-lactone and 10-hydroxy-CPT-carboxylate for both qualitative and quantitative analysis [11]. In addition to the continuous monitoring capabilities of this method, unlike other chromatography methods that require protein precipitation prior to analysis, the current method allowed real-time monitoring of CPT hydrolysis in the presence of HSA.

The real-time monitoring of CPT-lactone hydrolysis of CPT (Figs. 3a and 3b) pointed out that, first, the CPT-lactone hydrolysis rate increases exponentially with temperature, second, the almost perfect fit of the raw data using Eq. (1) signifies a unimolecular reaction and, third and most importantly, being a symptom of temperature-dependent lactone destabilization, the apparent equilibrium constant K'_h of the hydrolysis reaction increases with temperature.

The energy of activation E_a and the frequency factor A were determined from the slope and intercept of the corresponding linear fits of the Arrhenius plots shown in Fig. 3b. As Table I indicates, the average E_a for the hydrolysis reaction is $90.58 \text{ kJ mol}^{-1}$ and is somewhat higher than the energy barrier of the lactonization reaction ($81.12 \text{ kJ mol}^{-1}$). The higher energy of activation of the hydrolysis reaction is due to a much faster increase of the k_f with temperature as compared to the k_r . More specifically, k_f is only 5.05 times larger than k_r at $T = 304.15 \text{ K}$ as compared to being 6.62 times higher at $T = 329.15 \text{ K}$ (Table II).

Although the energy of activation for the hydrolysis and lactonization reactions is similar, the frequency factor A , which denotes the fraction of molecules colliding in the right orientation, is on average 225 times higher for the forward direction when compared to the reverse direction of the hydrolysis reaction and ~ 360 times higher for the reverse direction of the lactonization reaction. These results are very important for the following reasons: First, the very high values of the temperature-independent frequency factor are supportive of the unimolecular nature of the CPT-lactone

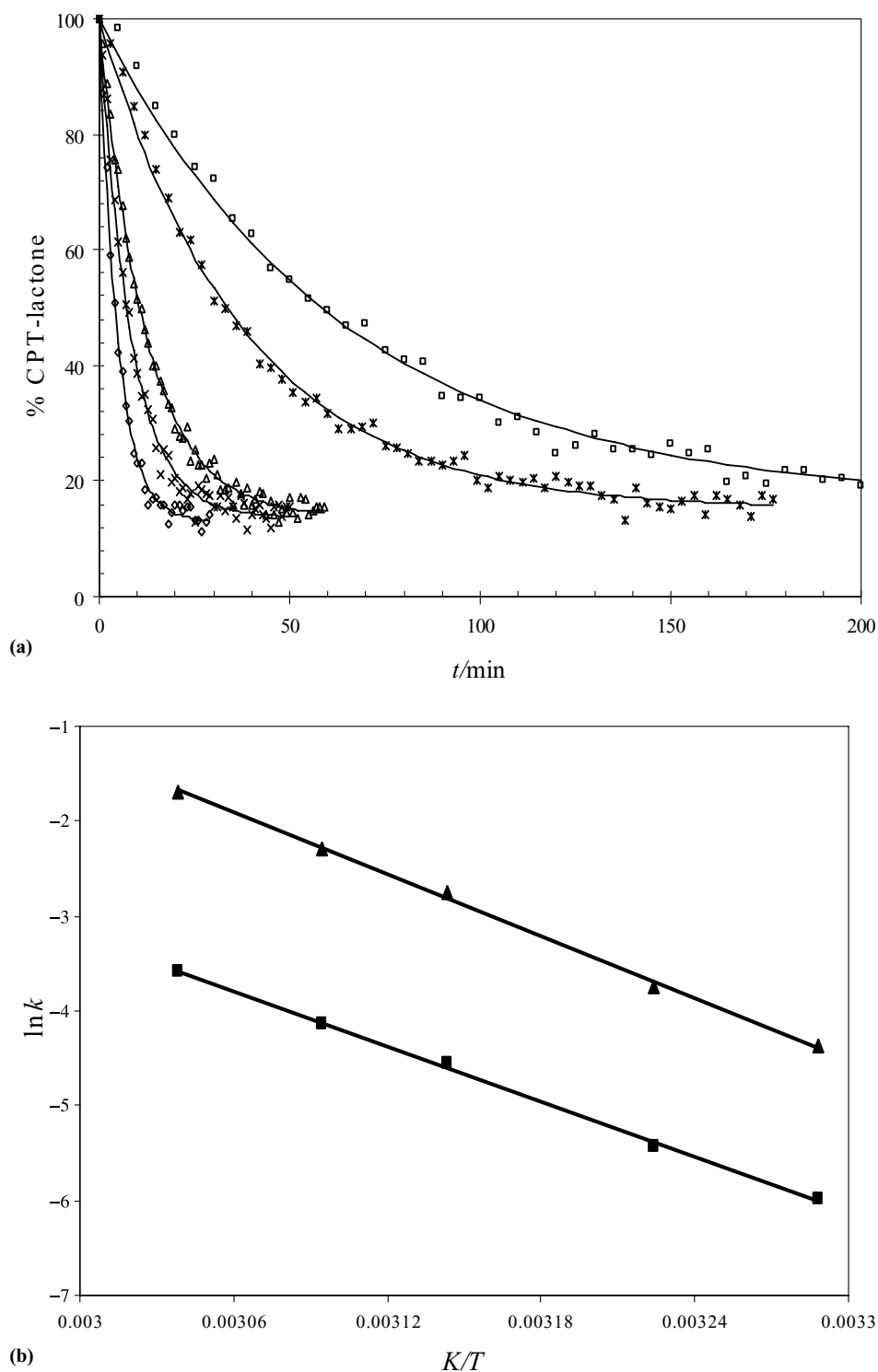


Figure 3 (a) Hydrolysis reaction kinetics of CPT-lactone at pH 7.4 and various temperatures: 304.15 K (□), 310.15 K (✱), 318.15 K (△), 323.15 K (×), and 329.15 K (◇). Solid lines refer to the simulated hydrolysis kinetics profile with fitting parameters derived as described in the methods section. (b) Linear fits of Arrhenius plots of $\ln k_f$ (▲) and $\ln k_r$ (■) as a function of the inverse of the temperature.

Table I Activation Energy and Preexponential Factor for the Hydrolysis and Lactonization Reactions for CPT-Lactone and CPT-Carboxylate

Reaction Direction	Hydrolysis Reaction		Lactonization Reaction	
	E_a (kJ mol ⁻¹)	10 ¹¹ A (min ⁻¹)	E_a (kJ mol ⁻¹)	10 ¹⁰ A (min ⁻¹)
Overall	89.18 ± 0.84	320.5 ± 107	86.49 ± 2.7	149.9 ± 135
Forward	90.58 ± 0.96	471.1 ± 179	76.61 ± 3.7	0.58 ± 0.4
Reverse	81.12 ± 0.37	2.10 ± 0.2	88.09 ± 2.6	232.9 ± 207

Energy of activation (E_a) and frequency factor (A) are reported as the mean ± standard deviation of three independent experiments. Overall, forward, and reverse directions are defined by the k_{obs} and k'_{obs} , k_f and k'_f and k_r and k'_r , respectively.

Table II First-Order Rate Constants Reported as the Mean ± SD of Three Experiments for Hydrolysis and Lactonization Reactions

T (K)	Hydrolysis Reaction			Lactonization Reaction		
	k_{obs} (min ⁻¹)	k_f (min ⁻¹)	k_r (min ⁻¹)	k'_{obs} (min ⁻¹)	k'_r (min ⁻¹)	k'_f (min ⁻¹)
304.15	0.0151 ± 0.0005	0.0126 ± 0.0004	0.00250 ± 0.0001	0.0157 ± 0.0003	0.0132 ± 0.0003	0.00250 ± 0.0001
310.15	0.0279 ± 0.0016	0.0235 ± 0.0013	0.00440 ± 0.0003	0.0282 ± 0.0024	0.0239 ± 0.0021	0.00430 ± 0.0005
318.15	0.0745 ± 0.0073	0.0640 ± 0.0067	0.0105 ± 0.0007	0.0650 ± 0.0026	0.0558 ± 0.0020	0.00920 ± 0.0006
323.15	0.117 ± 0.0044	0.101 ± 0.0042	0.0160 ± 0.0005	0.117 ± 0.0060	0.102 ± 0.0056	0.0150 ± 0.0013
329.15	0.213 ± 0.013	0.185 ± 0.012	0.0280 ± 0.0014	0.204 ± 0.012	0.179 ± 0.0089	0.0246 ± 0.0032

hydrolysis since orientation of the colliding molecules does not play a critical role. Second, the much higher frequency factor of the hydrolysis as compared to that of the lactonization reaction, coupled to the similar energetic barrier characterizing both reactions, suggests that the greater flexibility of the E-ring of the CPT-carboxylate is the reason for the less efficient lactonization of the hydrolyzed CPT.

These conclusions are also supported by Fig. 4, which depicts the kinetics of the esterification reaction with the CPT-carboxylate as the starting material. As expected, at lower temperatures the esterification reaction slows down, while in agreement with Fig. 3a, lactonization is favored at lower temperatures. Furthermore, as indicated in Table I, the E_a for the reverse direction of the hydrolysis reaction is slightly higher than that of the forward direction of the esterification reaction (81.12 ± 0.37 vs. 76.61 ± 3.7 kJ mol⁻¹). The small differences in the values calculated from the two experiments could be due to the small volume of DMSO used only during the study of the hydrolysis reaction as compared to the pure buffer solution used during the study of the lactonization reaction.

Values of the standard Gibbs free energy associated with the hydrolysis of CPT-lactone, calculated from $\Delta_r G'^{\circ}(T) = -RT \cdot \ln \{K'(T)\}$, are tabulated in Table III. The negative $\Delta_r G'^{\circ}(T)$ values indicate that the hydrolysis reaction is the thermodynamically stable reaction at pH 7.4. In addition, the decrease in $\Delta_r G'^{\circ}(T)$ values with increasing temperatures indi-

cates that hydrolysis of CPT-lactone is favorable at higher temperatures. The enthalpy, $\Delta_r H'^{\circ}(T)$, and entropy, $\Delta_r S'^{\circ}(T)$, associated with the hydrolysis reaction of CPT-lactone (9.90 ± 0.82 kJ mol⁻¹ and 43.30 ± 1.9 J K⁻¹ mol⁻¹, respectively) and the esterification of CPT-carboxylate (-11.55 ± 1.4 kJ mol⁻¹ and -51.56 ± 4.9 J K⁻¹ mol⁻¹, respectively) were determined from the slope and intercept of the linear fits of the plots of $\ln K'$ versus $1/T$ (Fig. 5). The detailed thermodynamic parameters are summarized in Table III. The positive value of enthalpy signified the endothermic nature of the hydrolysis. Interestingly, the positive entropy factor ($T \Delta_r S'^{\circ}(T)$) overcompensated the unfavorable enthalpic part for the hydrolysis reaction, yielding a negative $\Delta_r G'^{\circ}(T)$. In contrast, the chemical equilibrium constant K'_l for the lactonization reaction decreased with increasing temperatures, indicative of an exothermic reaction, but yet not spontaneous due to a large negative $\Delta_r S'^{\circ}(T)$, as reflected in the positive values of $\Delta_r G'^{\circ}(T)$. The similarity of these results with the published hydrolysis kinetics results of 10-hydroxy camptothecin strongly advocates that A-ring substitutions do not affect the stability of the E-ring [11,12].

The stability of CPT in the presence of 3.008 × 10⁻⁴ M HSA deteriorates as indicated by the shorter half-life ($t_{1/2}$) and reduced levels of equilibrium CPT-lactone concentration. More specifically, the $t_{1/2}$ and percent [CPT-lactone]_{eq} were found to be 13.1 min and 1.4%, respectively, as compared to 24.9 min and

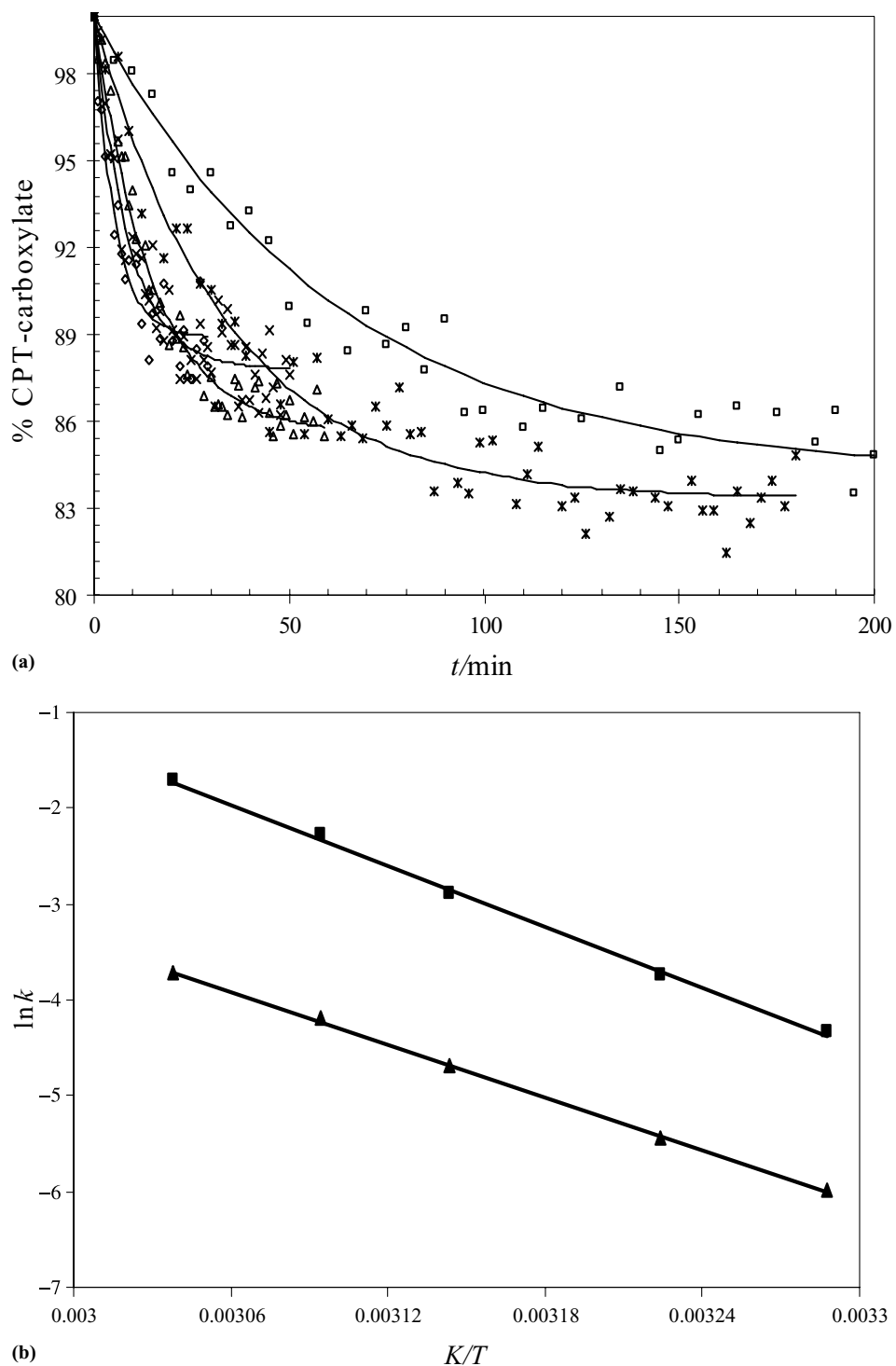


Figure 4 (a) Lactonization reaction kinetics of CPT-carboxylate at pH 7.4 and temperatures: 304.15 K (□), 310.15 K (*), 318.15 K (Δ), 323.15 K (×), and 329.15 K (◇). Solid lines refer to the simulated lactonization kinetics profile with fitting parameters derived as described in the methods section. (b) Linear fits of Arrhenius plots of $\ln k'_f$ (▲) and $\ln k'_r$ (■) as a function of the inverse of the temperature.

Table III Thermodynamic Parameters for the CPT-Lactone Hydrolysis, CPT-Carboxylate Lactonization, and Combined Average Values of the Thermodynamically Favored Hydrolysis Reaction

Hydrolysis reaction				
<i>T</i> (K)	% [CPT-lactone] _{eq}	% [CPT-carboxylate] _{eq}	<i>K'</i> _{<i>h</i>}	$\Delta_r G'^{\circ}(T)$ (kJ mol ⁻¹)
304.15	16.53	83.47	5.052 ± 0.039	-4.096 ± 0.024
310.15	15.73	84.27	5.367 ± 0.24	-4.330 ± 0.14
318.15	14.14	85.86	6.090 ± 0.44	-4.774 ± 0.20
323.15	13.61	86.39	6.355 ± 0.25	-4.966 ± 0.13
329.15	13.13	86.87	6.618 ± 0.15	-5.171 ± 0.075
$\Delta_r H'^{\circ} = 9.900 \pm 0.82$ kJ mol ⁻¹				
$\Delta_r S'^{\circ} = 43.30 \pm 1.9$ J K ⁻¹ mol ⁻¹				
Lactonization reaction				
<i>T</i> (K)	% [CPT-lactone] _{eq}	% [CPT-carboxylate] _{eq}	<i>K'</i> _{<i>l</i>}	$\Delta_r G'^{\circ}(T)$ /(kJ mol ⁻¹)
304.15	16.03	83.97	0.191 ± 0.008	4.188 ± 0.11
310.15	15.32	84.68	0.181 ± 0.017	4.413 ± 0.24
318.15	14.18	85.82	0.165 ± 0.006	4.762 ± 0.094
323.15	12.81	87.19	0.147 ± 0.014	5.159 ± 0.26
329.15	12.04	87.96	0.137 ± 0.013	5.450 ± 0.26
$\Delta_r H'^{\circ} = -11.55 \pm 1.4$ kJ mol ⁻¹				
$\Delta_r S'^{\circ} = -51.56 \pm 4.9$ J K ⁻¹ mol ⁻¹				
Combined average parameters for the thermodynamically favored hydrolysis reaction				
<i>T</i> (K)			<i>K'</i> _{<i>h</i>}	$\Delta_r G'^{\circ}(T)$ (kJ mol ⁻¹)
304.15			5.147 ± 0.18	-4.142 ± 0.08
310.15			5.460 ± 0.38	-4.372 ± 0.18
318.15			6.072 ± 0.31	-4.768 ± 0.14
323.15			6.599 ± 0.52	-5.063 ± 0.21
329.15			6.983 ± 0.61	-5.310 ± 0.23
$\Delta_r H'^{\circ} = 10.49 \pm 1.6$ kJ mol ⁻¹				
$\Delta_r S'^{\circ} = 48.00 \pm 5.4$ J K ⁻¹ mol ⁻¹				

Average apparent equilibrium constant at the corresponding temperature calculated at the mean of *K'* (forward direction) and 1/*K'* (reverse direction).

15.7% in the absence of HSA, at pH 7.4 and 310.15 K (Fig. 6). Furthermore, unlike the hydrolysis of CPT-lactone alone, in the presence of HSA the equilibrium lactone concentration does not change with temperature (Fig. 7a). The activation energy (*E_a*) and frequency factor (*A*) of CPT-lactone hydrolysis in the presence of HSA were determined from the dependence of rate constants (*k*) on temperature using the Arrhenius equation (Fig. 7b and Table IV). Interestingly, the *E_a* of CPT-lactone hydrolysis in the presence of HSA was found to be similar to that of the hydrolysis reaction of CPT-lactone alone at pH 7.4. The equilibrium of the hydrolysis reaction completely shifted toward the CPT-carboxylate with a loss of the reversibility of the reaction. The *k_{obs}* and equilibrium CPT concentrations at 310.15 K are in close agreement with previously reported kinetic analysis using HPLC as the analytical method [7–8,15–17].

To further investigate the mechanism of hydrolysis of CPT in the presence of HSA, we have carried out quantum yield measurements of the two species in the presence and absence of HSA under physiological pH

Table IV First-Order Rate Constants and Energy of Activation for Hydrolysis of CPT in the Presence of HSA, Reported as the Mean ± SD of Two Independent Experiments

<i>T</i> (K)	<i>k_{obs}</i> (min ⁻¹)	% [CPT-carboxylate] _{eq}
298.15	0.0135 ± 0.0001	99.8 ± 0.23
302.15	0.0209 ± 0.0013	99.7 ± 0.46
306.15	0.0311 ± 0.0004	98.3 ± 0.20
310.15	0.0526 ± 0.0010	98.6 ± 0.12
314.15	0.0673 ± 0.0027	98.9 ± 0.54

$$E_a = 80.66 \pm 0.39 \text{ kJ mol}^{-1}$$

$$A = (1.85 \pm 0.33) 10^{12} \text{ min}^{-1}$$

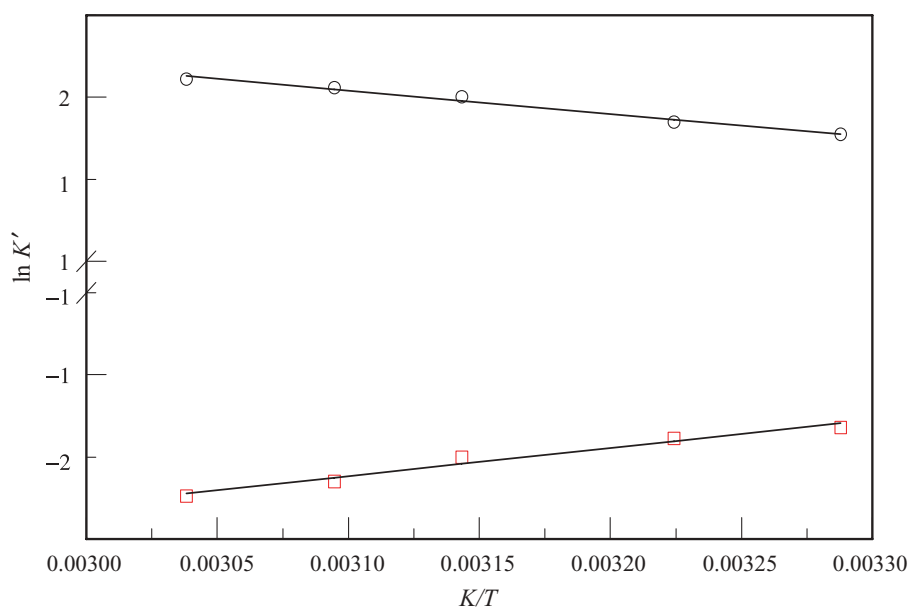


Figure 5 Van't Hoff plots depicting the temperature dependence of the apparent equilibrium hydrolysis constant K'_h (○) and apparent equilibrium lactonization constant K'_l (□). The relationship between $\ln K'$ and $(T/K)^{-1}$ was linear with $r^2 > 0.985$. $\Delta_r H'^{\circ}(T)$ and $\Delta_r S'^{\circ}(T)$ were calculated from the slope and intercept values of Eq. (5) as described in the methods section. [Color figure can be viewed in the online issue, which is available at www.interscience.wiley.com.]

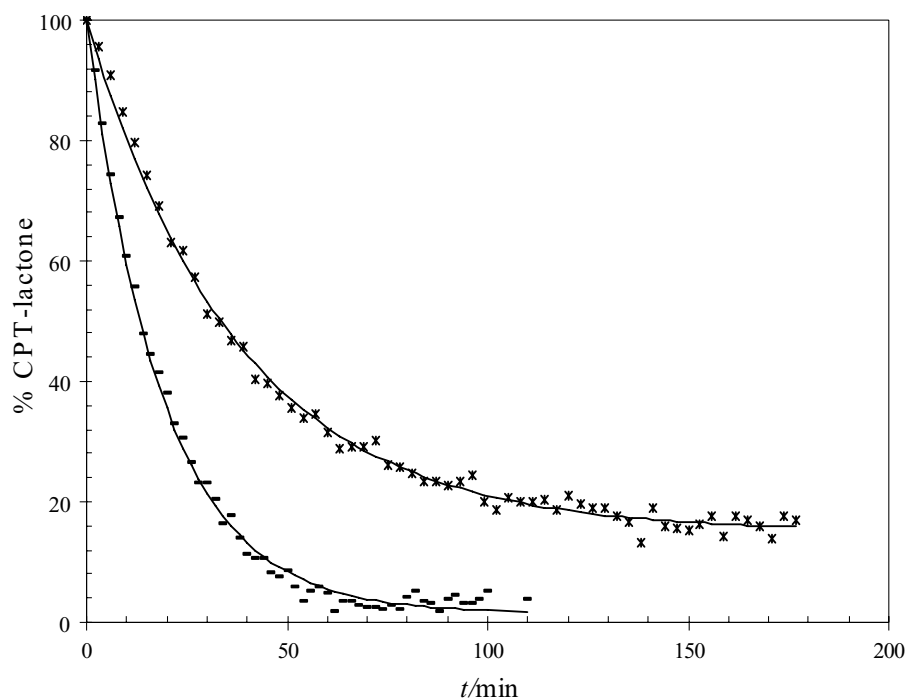


Figure 6 Hydrolysis kinetics of CPT-lactone at pH 7.4 and temperature 310.15 K in the presence (—) or absence (*) of HSA.

conditions. To avert species interconversion during the study, all readings were obtained within 10–20 s, and to ensure rapid binding of CPT molecules on the protein, HSA was used in great excess at a molar ratio of HSA to CPT ranging from 30/1 to 240/1.

As shown in Table V, fluorescence quantum yields of the CPT-lactone and CPT-carboxylate in PBS were found to be almost identical, indicating that light absorption and emission capacities of CPT in PBS are not affected by the status of the E-ring of the molecule.

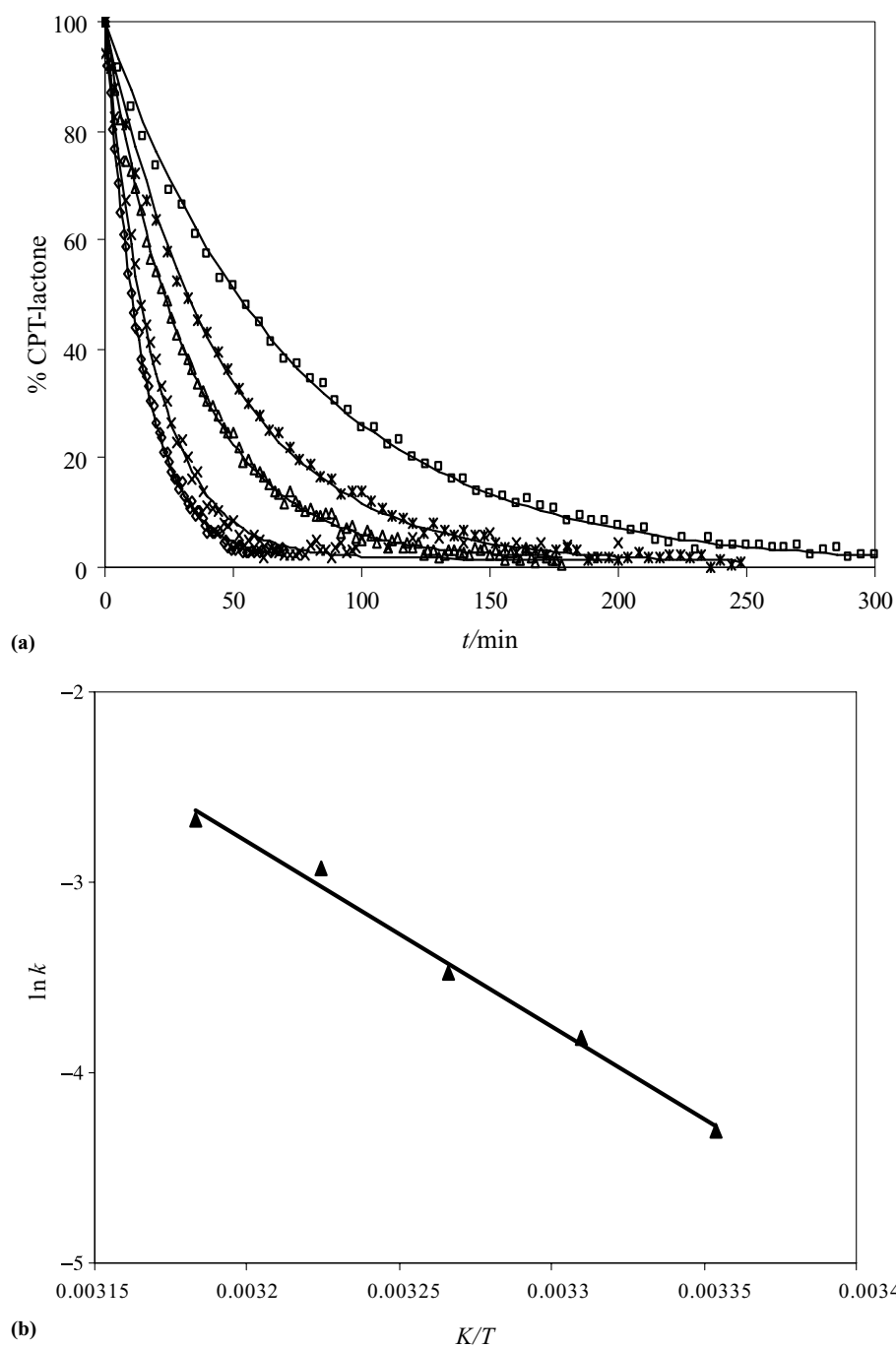


Figure 7 (a) Hydrolysis kinetics of CPT-lactone in the presence of HSA at pH 7.4 and various temperatures: 298.15 K (□), 302.15 K (✱), 306.15 K (△), 310.15 K (×), and 314.15 K (◇). Solid lines are the fitted data. (b) Arrhenius plot of the apparent hydrolysis rate constant k_{obs} of the CPT-lactone in the presence of HSA.

Contrary to that, due to the close proximity of CPT chromophore groups to HSA, significant quenching in quantum yield for both the species was observed in the presence of HSA. Interestingly, the reduction of quantum yield was approximately three times for

CPT-carboxylate but only ~ 2 times for CPT-lactone. More specifically, upon excitation at 350 nm, absorption of CPT-lactone in the presence of HSA was on average reduced by 23.4% as compared to a 29.7% reduction of the CPT-carboxylate. Similarly, integrated

Table V Fluorescence Quantum Yield of CPT-Lactone and CPT-Carboxylate in Presence and Absence of 0.020 g cm⁻³ HSA in PBS Buffer at pH 7.4 and 298.15 K, Reported as the Mean \pm SD of Two Independent Experiments

	PBS	PBS + HSA
CPT-lactone	0.719 \pm 0.007	0.377 \pm 0.011
CPT-carboxylate	0.708 \pm 0.009	0.233 \pm 0.003

fluorescence intensity of the CPT-lactone was reduced by 59.9% as compared to a 77.1% reduction of CPT-carboxylate. When the study was conducted using an excitation wavelength of 370 nm, the absorption intensity of both species in the presence of HSA was similarly reduced by 5.5% most probably because 370 nm is closer to the λ_{max} , of both CPT species. However, the integrated fluorescence of CPT-carboxylate was disproportionately reduced by 73.4% as compared to a 63.1% reduction of the CPT-lactone. Nonetheless, the calculated quantum yield of both species from both studies was practically identical. The find that CPT-carboxylate undergoes nonradiative relaxation to a higher extent, coupled with the higher affinity of CPT-carboxylate for HSA [8,15,16], supports the mechanistic explanation that HSA does not catalyze the hydrolysis reaction of CPT-lactone, but it rather binds, sequesters, and stabilizes the CPT-carboxylate species thus shifting the lactone-carboxylate equilibrium to the right.

BIBLIOGRAPHY

1. Wall, M. E.; Wani, M. C.; Nicholas, A. W.; Manikumar, G.; Tele, C.; Moore, L.; Trursdale, A.; Leitner, P.; Besterman, J. M. *J Med Chem* 1993, 36, 2689–2700.
2. Bruke, T. G.; Staubus, A. E.; Mishra, A. K. *J Am Chem Soc* 1992, 114, 8318–8319.
3. Euveni, D.; Halperin, D.; Shalit, I.; Priel, E.; Fabian, I. *Biochem Pharmacol* 2008, 75, 1272–1281.
4. Sriram, D.; Yogeewari, P.; Thirumurugan, R.; Bal, T. R. *Nat Prod Res* 2005, 19, 398–412.
5. Garcia-Carbonero, R.; Supko, J. *Clin Cancer Res* 2002, 8, 641–661.
6. Selvi, B.; Patel, S.; Savva, M. *J Pharm Sci* 2008, 97, 4379–4390.
7. Burke, T. G.; Mishra, A. K.; Wani, M. C.; Wall, M. E. *Biochemistry* 1993, 32, 5352–5364.
8. Burke, T. G.; Mi, Z. *J Med Chem* 1994, 37, 40–46.
9. Chourpa, I.; Millot, J.; Sockalingum, G. D.; Riou, J. Manfait, M. *Biochim Biophys Acta* 1998, 1379, 353–366.
10. Mi, Z.; Burke, T. G. *Biochemistry* 1994, 33, 10325–10336.
11. Kunadharaju, S.; Savva, M. *J Chem Thermo* 2008, 40, 1439–1444.
12. Fassberg, J.; Stella, V. J. *J Pharm Sci* 1992, 81, 676–684.
13. Dey, J.; Warner, I. M. *J Lumin* 1997, 71, 105–114.
14. Parker, C. A.; Rees, W. T. *Analyst* 1966, 85, 587–600.
15. Burke, T. G.; Mi, Z. *Anal Biochem* 1993, 212, 285–287.
16. Mi, Z.; Burke, T. G. *Biochemistry* 1994, 33, 12540–12545.
17. Mi, Z.; Malak, H.; Burke, T. G. *Biochemistry* 1995, 34, 13722–13728.